Tradeoffs in Stochastic Event-Triggered Control

Burak Demirel, Alex S. Leong, Vijay Gupta, and Daniel E. Quevedo

***Abstract*—This paper studies the optimal output-feedback control of a linear time-invariant system where a stochastic event-based scheduler triggers the communication between the sensor and the controller. The primary goal of the use of this type of scheduling strategy is to provide significant reductions in the usage of the sensor-to-controller communication and, in turn, improve energy expenditure in the network. In this paper, we aim to design an admissible control policy, which is a function of the observed output, to minimize a quadratic cost function while employing a stochastic event-triggered scheduler that preserves the Gaussian property of the plant state and the estimation error. For the infinite horizon case, we present analytical expressions that quantify the tradeoff between the communication cost and control performance of such event-triggered control systems. This tradeoff is confirmed quantitatively via numerical examples. Besides, numerical simulations justify that the event-triggered control provides better quadratic control performance than the (traditional) periodic time-triggered control at the same average sampling rate.**

***Index Terms*—Event-triggered control, linear systems, optimal control, stochastic control.**

I. Introduction

Over the past decade, distributed control and estimation over networks have been a major trend. Thanks to the forthcoming revolution of the Internet-of-Things and resulting interconnectedness of smart technologies, the importance of decision making over communication networks grows ever larger in our modern society. These technological advances, however, bring new challenges regarding how to use the limited computation, communication, and energy resources efficiently. Consequently, event- and self-triggered algorithms have appeared as an alternative to traditional time-triggered algorithms in both estimation and control (see, e.g., [1]).

A vast majority of the research in this area has mainly focused on proving the stability of the proposed control schemes, and demonstrating the effectiveness of such control systems, as compared to periodically sampled ones, through numerical simulations. However, an important stream of work in such schemes is analytically characterizing the tradeoff between the control performance and communication rate (or sampling interval) achieved via these algorithms (see, e.g., [2]–[9]). The authors of [10] investigated the minimum-variance event-triggered output-feedback control problem, (cf., [2]). They established a separation between the control strategy and the scheduling decision, and they also showed that scheduling decisions are determined by solving an optimal stopping problem.

Optimal event-triggered control design requires the joint optimal design of the controller and the scheduler. The associated optimization problem becomes notoriously difficult [11] since, in general, the controller and the scheduler have different information. A vast majority of work in the literature focuses on the design of optimal feedback control laws for a predefined scheduling rule. It is important to note that designing an optimal control law might be very complicated even if one considers a fixed event-triggering policy. For instance, our recent work [12] shows that, even for linear time-invariant (LTI) systems, the quadratic optimal control problem, where a threshold-based event-triggered mechanism is used to decide if there is a need for transmission of new control actions based on knowledge of the plant state, leads to a nonconvex optimization problem.

The selection of the event-triggering mechanism is essential for the computation of the control performance. As noted in [9], in the case of Gauss–Markov plant models, due to the use of a (deterministic) threshold-based triggering mechanism, the plant state becomes a truncated Gaussian variable. As a result, computation of the control performance becomes challenging since it requires calculating the covariance of the plant state via numerical methods. One way to tackle this problem consists in employing a stochastic triggering mechanism,[1] which preserves the Gaussianity of the plant state, as proposed in [13]–[15]. Our initial work in [16] used a deadbeat controller and a stochastic scheduler, which is similar to the one introduced in [13], to quantify the tradeoff between the communication and the control cost for scalar systems. Similarly, Brunner *et al.* [17] proposed an event-triggered control scheme that works under stochastic triggering rules. They also derived a control policy that always outperforms a periodic one. Differing from [17], in this paper, we will focus on solving the optimal output event-triggered control problem.

Contributions. In this paper, we consider optimal output-feedback control of an LTI system where a stochastic event-based triggering algorithm uses information on current state estimation errors to dictate the communication between the smart sensor and the controller. The proposed scheduler decides at each time step whether or not to transmit new state estimates from the sensor to the controller based on state estimation errors. The main contributions of this manuscript are as follows.

1) We develop a framework for quantifying the closed-loop control performance and the communication rate in the channel between the sensor and the controller.
2) We confirm that the certainty-equivalent controller is optimal under the proposed scheduling rule. Our previous work [9] used a transmission strategy based on the plant state, and employed a sequence of deadbeat control actions to establish a resetting property, but this

Manuscript received March 3, 2018; revised July 18, 2018; accepted August 19, 2018. Date of publication September 26, 2018; date of current version May 27, 2019. Recommended by Associate Editor Z. Gao. *(Corresponding author: Burak Demirel.)*

B. Demirel, A. S. Leong, and D. E. Quevedo are with the Chair of Automatic Control (EIM-E), Paderborn University, Paderborn 33098, Germany (e-mail: burak.demirel@protonmail.com; alex.leong@upb.de; dquevedo@ieee.org).

V. Gupta is with the Department of Electrical Engineering, University of Notre Dame, Notre Dame, IN 46556 USA (e-mail: vgupta2@nd.edu).

Color versions of one or more of the figures in this paper are available online at http://ieeexplore.ieee.org.

Digital Object Identifier 10.1109/TAC.2018.2872199

[1]The use of a stochastic triggering mechanism provides slightly worse performance than the use of a deterministic one due to the additional uncertainty introduced by randomness in the triggering decisions.

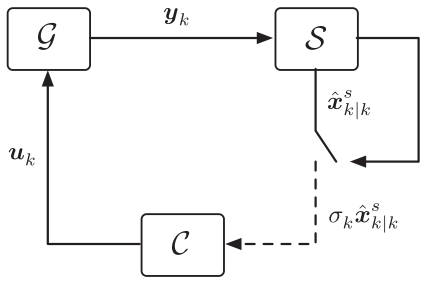

Fig. 1. Block diagram of a feedback control system with plant $\mathcal{G}$, sensor/scheduler $\mathcal{S}$, and controller $\mathcal{C}$. The solid line represents an ideal channel, whereas the dashed line indicates a resource-constrained channel.

was not optimal since the separation principle between control and scheduling does not hold.

3) We derive analytical expressions for the (average) communication rate and control performance. Our analysis relies on a Markov chain characterization of the evolution of the state prediction error (cf., [9]) where the states of this Markov chain describe the time elapsed since the last transmission.
4) Due to the use of the stochastic triggering rule, we can compute the conditional covariance of the comparison error (i.e., the difference between the state estimation error at the sensor and the state estimation error at the controller) in a closed form. Consequently, it becomes almost effortless to compute the closed-loop control performance (cf., [9]).

Outline. Section II describes the system architecture and formulates an optimal event-triggered control problem. Section III verifies the optimality of the certainty equivalent control law in the presence of the event-based communication. This section also presents analytic expressions of the communication rate and the control performance for the infinite horizon problem. An illustrative example is presented to demonstrate the tradeoff between communication and control performance in Section IV. Section V gives concluding remarks.

Nomenclature. The set of all real symmetric positive semi-definite matrices of dimension n is denoted by $\mathbb{S}^n_{\succeq 0}$. The inner product of two vectors $\boldsymbol{u}$ and $\boldsymbol{v}$ is denoted by $\langle \boldsymbol{u}, \boldsymbol{v} \rangle$.

II. Problem Formulation

Control architecture: The feedback control system, depicted in Fig. 1, is considered. A physical plant $\mathcal{G}$, whose dynamics can be represented by a stochastic LTI system, is being controlled. A battery-powered sensor $\mathcal{S}$ takes samples of the plant output $\boldsymbol{y}_k$ and transmits the estimate of the plant state $\boldsymbol{x}_k$ to the controller over a resource-constrained communication channel. To tackle the resource constraint, the sensor employs an event-based scheduler, that makes a transmission decision by comparing its estimate of the plant state with the estimate at the controller. The controller $\mathcal{C}$ computes new control actions based on the available information. Whenever the controller receives a new state estimate from the sensor, it calculates a control command based on this state estimate. Otherwise, it runs an estimator to predict the plant state, and it uses this information to calculate a new control action. In this context, we are interested in deriving analytical performance guarantees, both regarding the control performance and the number of transmissions between the sensor and the controller.

Plant model. The plant $\mathcal{G}$ is modeled as a discrete-time LTI system

$$\boldsymbol{x}_{k+1} = A\boldsymbol{x}_k + B\boldsymbol{u}_k + \boldsymbol{w}_k \tag{1}$$

driven by the control input $\boldsymbol{u}_k \in \mathbb{R}^m$ (calculated by the controller $\mathcal{C}$), and an unknown noise process $\boldsymbol{w}_k \in \mathbb{R}^n$. The state $\boldsymbol{x}_k \in \mathbb{R}^n$ is available only indirectly through the noisy output measurement

$$\boldsymbol{y}_k = C\boldsymbol{x}_k + \boldsymbol{v}_k. \tag{2}$$

The two noise sources $\boldsymbol{w}_k \in \mathbb{R}^n$ and $\boldsymbol{v}_k \in \mathbb{R}^p$ are assumed to be uncorrelated zero-mean Gaussian white-noise random processes with covariance matrices $W \in \mathbb{S}^n_{\succeq 0}$ and $V \in \mathbb{S}^p_{\succ 0}$, respectively. We refer to $\{\boldsymbol{w}_k\}_{k \geq 0}$ as the process noise, and to $\{\boldsymbol{v}_k\}_{k \geq 0}$ as the measurement noise. The initial state $\boldsymbol{x}_0$ is modeled as a Gaussian distributed random variable with mean $\bar{\boldsymbol{x}}_0$ and covariance $X_0 \in \mathbb{S}^n_{\succeq 0}$. We assume that the pairs (A, B) and $(A, W^{1/2})$ are controllable, where $W^{1/2}$ is the Cholesky[2] factor of W, while the pair (A, C) is observable.

Smart sensor, preprocessor, and scheduler: Using a standard Kalman filter, the sensor locally computes *minimum mean squared error* (MMSE) estimates $\hat{\boldsymbol{x}}^s_{k|k}$ of the plant state $\boldsymbol{x}_k$ based on the information available to the sensor at time k, and transmits them to the controller. As noted in [18] and [19], sending state estimates, in general, provides better performance than transmitting measurements. The sensor also employs a transmission scheduler, which decides whether or not to send the current state estimate to the controller at each time step $k \in \mathbb{N}_0$ as determined by

$$\sigma_k = \begin{cases} 1, & \text{if MMSE estimate } \hat{\boldsymbol{x}}^s_{k|k} \text{ is sent} \\ 0, & \text{otherwise.} \end{cases} \tag{3}$$

Assumption 1: The sensor $\mathcal{S}$ has precise knowledge of the control policy used to generate control actions, which are computed by the controller and applied by the actuator to the plant. Hence, the information set of the smart sensor $\mathcal{S}$ contains all controls used up to time $k-1$.

The information set available to the sensor at time $k \in \mathbb{N}_0$ is

$$\mathcal{I}^s_k \triangleq \{\sigma_0, \ldots, \sigma_{k-1}; \boldsymbol{y}_0, \ldots, \boldsymbol{y}_k; \boldsymbol{u}_0, \ldots, \boldsymbol{u}_{k-1}\}. \tag{4}$$

The MMSE estimate $\hat{\boldsymbol{x}}^s_{k|k}$ of the plant state $\boldsymbol{x}_k$ can be computed recursively starting from the initial condition $\hat{\boldsymbol{x}}^s_{0|-1} = \bar{\boldsymbol{x}}_0$ and $P^s_{0|-1} = X_0$ by using a Kalman filter [20]. At this point, it is worth reviewing the fundamental equations underlying the Kalman filter algorithm. The algorithm consists of two steps.

1) *Prediction step:* This step predicts the state, estimation error, and estimation error covariance at time k dependent on information at time $k-1$

$$\hat{\boldsymbol{x}}^s_{k|k-1} \triangleq \mathbf{E}\left[\boldsymbol{x}_k \mid \mathcal{I}^s_{k-1}\right] = A\hat{\boldsymbol{x}}^s_{k-1|k-1} + B\boldsymbol{u}_{k-1} \tag{5}$$

$$\tilde{\boldsymbol{x}}^s_{k|k-1} \triangleq \boldsymbol{x}_k - \hat{\boldsymbol{x}}^s_{k|k-1} = A\tilde{\boldsymbol{x}}^s_{k-1|k-1} + \boldsymbol{w}_{k-1} \tag{6}$$

$$P^s_{k|k-1} \triangleq \mathbf{E}\left[\tilde{\boldsymbol{x}}^s_{k|k-1}\tilde{\boldsymbol{x}}^{s\top}_{k|k-1} \mid \mathcal{I}^s_{k-1}\right] = AP^s_{k-1|k-1}A^\top + W. \tag{7}$$

2) *Update step:* This step updates the state, estimation error, and estimation error covariance using a blend of the predicted state and the observation $\boldsymbol{y}_k$

$$\hat{\boldsymbol{x}}^s_{k|k} \triangleq \mathbf{E}\left[\boldsymbol{x}_k \mid \mathcal{I}^s_k\right] = \hat{\boldsymbol{x}}^s_{k|k-1} + K_k\left(\boldsymbol{y}_k - C\hat{\boldsymbol{x}}^s_{k|k-1}\right) \tag{8}$$

$$\tilde{\boldsymbol{x}}^s_{k|k} \triangleq \boldsymbol{x}_k - \hat{\boldsymbol{x}}^s_{k|k} = (\mathbf{I}_n - K_kC)A\tilde{\boldsymbol{x}}^s_{k-1|k-1} + (\mathbf{I}_n - K_kC)\boldsymbol{w}_{k-1} - K_k\boldsymbol{v}_k \tag{9}$$

$$P^s_{k|k} \triangleq \mathbf{E}\left[\tilde{\boldsymbol{x}}^s_{k|k}\tilde{\boldsymbol{x}}^{s\top}_{k|k} \mid \mathcal{I}^s_k\right] = (\mathbf{I}_n - K_kC)\,P^s_{k|k-1} \tag{10}$$

where the gain matrix is given by

$$K_k \triangleq P^s_{k|k-1}C^\top\left(CP^s_{k|k-1}C^\top + V\right)^{-1}. \tag{11}$$

[2]Given a matrix $W \in \mathbb{S}^n_{\succeq 0}$, its Cholesky factor is an upper-triangular matrix $\mathcal{O}$ such that $\mathcal{O}\mathcal{O}^\top = W$.

It is worth noting that the estimation error at the sensor $\tilde{\boldsymbol{x}}^s_{k|k}$ is Gaussian with zero mean and covariance $P^s_{k|k}$, that evolves according to the standard Riccati recursion [21, Ch. 9]. Since the pair (A, C) is observable and the pair $(A, W^{1/2})$ is controllable, the matrices $P^s_{k|k-1}$ and K_k converge exponentially to steady state values P^s_∞ and K_∞, respectively. In consequence, the matrix $P^s_{k|k}$ also converges to a steady state value, i.e., $F^s_\infty \triangleq (\mathbf{I}_n - K_\infty C)P^s_\infty$.

The scheduler and the sensor are collocated, and the scheduler has access to all available information at the sensor. Moreover, the scheduler employs an event-based triggering mechanism to decide if there is a need for transmission of an updated state estimate from the sensor to the controller. The occurrence of information transmission is defined as

$$\sigma_k = \begin{cases} 1, & \text{if } \delta_k = 1 \text{ or } \tau_{k-1} = \mathrm{T} \\ 0, & \text{otherwise} \end{cases} \tag{12}$$

where δ_k is a (random) binary decision variable [which, in this paper, evolves according to (13)], τ_k is a nonnegative integer variable introduced to describe the time elapsed since the last transmission, and T is a time-out interval. Such a time-out mechanism is critical in event-triggered control systems to guard against faulty components (see, e.g., [9]). Not receiving any new messages on the controller side for a long time could be due to two reasons: either the triggering condition is not satisfied, or the sensor is not operational anymore.

To maintain the Gaussianity of the comparison error

$$\boldsymbol{e}_{k|k-1} \triangleq \hat{\boldsymbol{x}}^s_{k|k} - \hat{\boldsymbol{x}}^c_{k|k-1}$$

[note that $\hat{\boldsymbol{x}}^s_{k|k}$ is defined in (8) while $\hat{\boldsymbol{x}}^c_{k|k-1}$ is introduced in (17)] a variant of the stochastic triggering mechanism proposed in [13]–[15] is used. More specifically, the scheduler will decide to transmit a new sensor packet according to the following decision rule:

$$\delta_k = \begin{cases} 0, & \text{with prob. } e^{-\lambda\langle \boldsymbol{e}_{k|k-1}, \boldsymbol{e}_{k|k-1}\rangle} \\ 1, & \text{with prob. } 1 - e^{-\lambda\langle \boldsymbol{e}_{k|k-1}, \boldsymbol{e}_{k|k-1}\rangle} \end{cases} \tag{13}$$

where the triggering parameter λ is a given positive scalar (i.e., $0 < \lambda < \infty$). As can be seen in (13), the probability of transmitting a new sensor packet (i.e., $\sigma_k = 1$) converges to one as λ goes to infinity. In other words, for large values of λ, the communication between the sensor and the controller is more likely to be triggered.

The integer-valued random process $\{\tau_k\}_{k\geq 0}$ in (12) describes how many time instances ago the last transmission of a sensor packet occurred. Whenever a sensor packet is transmitted from the sensor to the controller, τ_k is reset to zero. Thus, the evolution of the random process $\{\tau_k\}_{k\geq 0}$ is defined by

$$\tau_k = \begin{cases} 0, & \text{if } \delta_k = 1 \text{ or } \tau_{k-1} = \mathrm{T} \\ 1 + \tau_{k-1}, & \text{otherwise} \end{cases} \tag{14}$$

or equivalently

$$\tau_k = \begin{cases} 0, & \text{if } \sigma_k = 1 \\ 1 + \tau_{k-1}, & \text{if } \sigma_k = 0 \end{cases} \tag{15}$$

where $\tau_{-1} = 0$. Notice that the number of time steps between two consecutive transmissions is bounded by the time-out interval $\mathrm{T} < \infty$. If the number of samples since the last transmission exceeds a time-out value of T, the sensor will attempt to transmit new data to the controller even if the comparison error does not satisfy the triggering condition (13). Thus, a transmission (i.e., $\sigma_k = 1$) will occur when either $\delta_k = 1$ or there is a time out.

Remark 2: It is worth noting that, as can be seen in (15), the events $\{\sigma_k = 1\}$ and $\{\tau_k = 0\}$ are equivalent to each other.

At time instances when $\sigma_k = 1$, the sensor transmits its local state estimate $\hat{\boldsymbol{x}}^s_{k|k}$ to the controller. As a result, the information set available to the controller at time $k \in \mathbb{N}_0$ (and before deciding upon $\boldsymbol{u}_k$) can be defined as

$$\mathcal{I}^c_k \triangleq \{\sigma_0, \ldots, \sigma_k; \sigma_0 \hat{\boldsymbol{x}}^s_{0|0}, \ldots, \sigma_k \hat{\boldsymbol{x}}^s_{k|k}; \boldsymbol{u}_0, \ldots, \boldsymbol{u}_{k-1}\}. \tag{16}$$

Under the event-based scheduling mechanism, (12)–(14), the controller runs an MMSE estimator to compute estimates of the plant state $\boldsymbol{x}_k$ recursively as

$$\hat{\boldsymbol{x}}^c_{k|k-1} \triangleq \mathbf{E}[\boldsymbol{x}_k \mid \mathcal{I}^c_{k-1}] = A\hat{\boldsymbol{x}}^c_{k-1|k-1} + B\boldsymbol{u}_{k-1} \tag{17}$$

$$\hat{\boldsymbol{x}}^c_{k|k} \triangleq \mathbf{E}[\boldsymbol{x}_k \mid \mathcal{I}^c_k] = \begin{cases} \hat{\boldsymbol{x}}^s_{k|k}, & \text{if } \sigma_k = 1 \\ \hat{\boldsymbol{x}}^c_{k|k-1}, & \text{otherwise} \end{cases} \tag{18}$$

starting from $\hat{\boldsymbol{x}}^c_{0|-1} = \bar{\boldsymbol{x}}_0$. Here, $\hat{\boldsymbol{x}}^c_{k|k-1}$ is the optimal estimate at the controller if the sensor did not transmit any information at time step $k \in \mathbb{N}_0$. Note that the optimality of this estimator can be shown by using a similar argument to that provided in [15, Lemma 4].

Assumption 3: In addition to computing $\hat{\boldsymbol{x}}^s_{k|k}$, the sensor operates another estimator, which mimics the one at the controller, since transmission decisions rely on both $\hat{\boldsymbol{x}}^s_{k|k}$ and $\hat{\boldsymbol{x}}^c_{k|k-1}$ [see (13)]. This can be done provided we make the following assumption.

Assumption 4: Both the smart sensor $\mathcal{S}$ and the controller $\mathcal{C}$ know the plant model $\mathcal{G}$ (but not realizations of the noise processes).

Controller design and performance criterion. We aim at finding the control strategies $\boldsymbol{u}_k$, as a function of the admissible information set $\mathcal{I}^c_k$ defined in (16), to minimize a quadratic cost function of the form

$$J_N = \mathbf{E}\left[\boldsymbol{x}_N^\top Q_f \boldsymbol{x}_N + \sum_{k=0}^{N-1} \left(\boldsymbol{x}_k^\top Q \boldsymbol{x}_k + \boldsymbol{u}_k^\top R \boldsymbol{u}_k\right)\right] \tag{19}$$

where $Q, Q_f \in \mathbb{S}^n_{\succeq 0}$ and $R \in \mathbb{S}^m_{\succ 0}$. The expectation is taken over the uncorrelated variables $\boldsymbol{x}_0$, $\{\boldsymbol{w}_k\}_{k\geq 0}$, and $\{\boldsymbol{v}_k\}_{k\geq 0}$. At time instances when $\sigma_k = 1$ (i.e., the controller has received sensor packets), the controller uses the state estimate $\hat{\boldsymbol{x}}^s_{k|k}$, which was transmitted by the sensor. However, at time instances when $\sigma_k = 0$, the controller uses the outcome of the estimator at the controller side. As is well known in related situations (e.g., [11], [22]), if the transmission decision σ_k is independent of the control strategy $\boldsymbol{u}_k$, then the certainty equivalent controller is optimal.

III. Main Results

We wish to quantify the communication rate and control performance of the feedback control system described by (1) and (2), where the event-based triggering mechanism (13) determines the communication between the sensor and the controller. We will first demonstrate that the time elapsed between two consecutive transmissions can be regarded as a discrete-time, finite state, and time-homogeneous Markov chain. Then, using an ergodicity property, we will provide an analytical formula for the communication rate between the sensor and the controller. Subsequently, we will show that the *certainty equivalent controller* is still optimal with the event-triggering rule (13). Finally, we will compute the control performance analytically for the infinite horizon case.

Assumption 5: In the rest of this paper, we will assume that the Kalman filter at the sensor runs in steady state. This means $P^s_{k|k-1}$ and K_k have reached their steady-state values P^s_∞ and K_∞.

We first define the state prediction error at the controller

$$\tilde{\boldsymbol{x}}^c_{k|k-1} \triangleq \boldsymbol{x}_k - \hat{\boldsymbol{x}}^c_{k|k-1} \tag{20}$$

which evolves as

$$\tilde{\boldsymbol{x}}^c_{k+1|k} = \begin{cases} A\tilde{\boldsymbol{x}}^s_{k|k} + \boldsymbol{w}_k, & \text{if } \sigma_k = 1 \\ A\tilde{\boldsymbol{x}}^c_{k|k-1} + \boldsymbol{w}_k, & \text{if } \sigma_k = 0. \end{cases} \tag{21}$$

Then, we define the state estimation error at the controller

$$\tilde{\boldsymbol{x}}^c_{k|k} \triangleq \boldsymbol{x}_k - \hat{\boldsymbol{x}}^c_{k|k} \tag{22}$$

which evolves as

$$\tilde{\boldsymbol{x}}^c_{k|k} = \begin{cases} \tilde{\boldsymbol{x}}^s_{k|k}, & \text{if } \sigma_k = 1 \\ A\tilde{\boldsymbol{x}}^c_{k-1|k-1} + \boldsymbol{w}_{k-1}, & \text{if } \sigma_k = 0. \end{cases} \tag{23}$$

Define also the comparison errors:

$$\boldsymbol{e}_{k|k-1} \triangleq \hat{\boldsymbol{x}}^s_{k|k} - \hat{\boldsymbol{x}}^c_{k|k-1} = \tilde{\boldsymbol{x}}^c_{k|k-1} - \tilde{\boldsymbol{x}}^s_{k|k} \tag{24}$$

$$\boldsymbol{e}_{k|k} \triangleq \hat{\boldsymbol{x}}^s_{k|k} - \hat{\boldsymbol{x}}^c_{k|k} = \tilde{\boldsymbol{x}}^c_{k|k} - \tilde{\boldsymbol{x}}^s_{k|k}. \tag{25}$$

Whenever a transmission occurs (i.e., $\tau_k = 0$), the state estimation error $\tilde{\boldsymbol{x}}^c_{k|k}$ at the controller is equal to $\tilde{\boldsymbol{x}}^s_{k|k}$, since the most recent sensor packet is available at the controller. It is then possible to write the stochastic recurrence (24) and (25) as

$$\boldsymbol{e}_{k+1|k} = \begin{cases} \boldsymbol{\eta}_k, & \text{if } \tau_k = 0 \\ A\boldsymbol{e}_{k|k-1} + \boldsymbol{\eta}_k, & \text{if } \tau_k \neq 0 \end{cases} \tag{26}$$

and

$$\boldsymbol{e}_{k|k} = \begin{cases} 0, & \text{if } \tau_k = 0 \\ A\boldsymbol{e}_{k-1|k-1} + \boldsymbol{\eta}_{k-1}, & \text{if } \tau_k \neq 0 \end{cases} \tag{27}$$

where $\boldsymbol{\eta}_k \triangleq K_\infty C(A\tilde{\boldsymbol{x}}^s_{k|k} + \boldsymbol{w}_k) + K_\infty \boldsymbol{v}_{k+1}$. Notice that the comparison errors $\boldsymbol{e}_{k|k-1}$ and $\boldsymbol{e}_{k|k}$ propagate according to a linear system with open-loop dynamics A, driven by the process $\boldsymbol{\eta}_k$.

Lemma 6: $\{\boldsymbol{\eta}_k\}_{k\geq 0}$ is a sequence of pairwise independent Gaussian random vectors such that $\boldsymbol{\eta}_k \sim \mathcal{N}(0, \Pi_\eta)$ with $\Pi_\eta \triangleq K_\infty C P^s_\infty$.

Remark 7: If the sensor has perfect state measurements (i.e., $\boldsymbol{y}_k = \boldsymbol{x}_k$), then $\boldsymbol{\eta}_k$ will be equal to $\boldsymbol{w}_k$.

Definition 8 (Cumulative error): We shall characterize the cumulative comparison error (i.e., the error that occurs in estimation at the controller over time due to intermittent transmissions) via

$$\boldsymbol{\epsilon}_k(i) \triangleq \sum_{j=0}^{i} A^j \boldsymbol{\eta}_{k-j}. \tag{28}$$

Using Definition 8, the stochastic recurrence (26) and (27) can be then rewritten as

$$\boldsymbol{e}_{k+1|k} = \boldsymbol{\epsilon}_k(\tau_k) \tag{29}$$

$$\boldsymbol{e}_{k|k} = \begin{cases} 0, & \text{if } \tau_k = 0 \\ \boldsymbol{\epsilon}_{k-1}(\tau_{k-1}), & \text{if } \tau_k \neq 0. \end{cases} \tag{30}$$

Lemma 9 (Augmented cumulative error vector): Consider $\bar{\boldsymbol{\epsilon}}_k(i) \triangleq \left[\boldsymbol{\epsilon}_k^\top(0)\ \boldsymbol{\epsilon}_{k+1}^\top(1)\ \cdots\ \boldsymbol{\epsilon}_{k+i}^\top(i)\right]^\top$ with $\boldsymbol{\epsilon}_k(i)$ as in (28). Then, $\bar{\boldsymbol{\epsilon}}_k(i)$ is a random vector having a multivariate normal distribution with zero mean and covariance

$$\Sigma_\epsilon(i) \triangleq \begin{bmatrix} \Pi_\eta & \Pi_\eta A^\top & \dots & \Pi_\eta (A^i)^\top \\ \star & \sum_{j=0}^{1} A^j \Pi_\eta (A^j)^\top & \dots & \sum_{j=0}^{1} A^j \Pi_\eta (A^{j+i-1})^\top \\ \vdots & \vdots & \ddots & \vdots \\ \star & \star & \dots & \sum_{j=0}^{i} A^j \Pi_\eta (A^j)^\top \end{bmatrix}$$

for any $i \in \{0, 1, \ldots, \mathrm{T}-1\}$ (Notice that $\Sigma_\epsilon(0) = \Pi_\eta$).

Lemma 10 (Markov chain): The sequence of random variables $\{\tau_k\}_{k\geq 0}$ is a homogeneous Markov chain with state space $\mathcal{B} = \{0, 1, \ldots, \mathrm{T}\}$ and the transition matrix

$$\mathsf{P} = \begin{bmatrix} p_{0,0} & 1-p_{0,0} & 0 & \dots & 0 \\ p_{1,0} & 0 & 1-p_{1,0} & \dots & 0 \\ \vdots & \vdots & \vdots & \ddots & \vdots \\ p_{\mathrm{T}-1,0} & 0 & 0 & \dots & 1-p_{\mathrm{T}-1,0} \\ p_{\mathrm{T},0} & 0 & 0 & \dots & 0 \end{bmatrix} \tag{31}$$

where the nonzero transition probabilities are computed as

$$p_{i,j} = \begin{cases} 1 - \dfrac{1}{\sqrt{|\mathbf{I}_n + 2\lambda\Sigma_\epsilon(0)|}}, & \text{if } i = 0,\ j = 0 \\ 1 - \sqrt{\dfrac{|\mathbf{I}_{in} + 2\lambda\Sigma_\epsilon(i-1)|}{|\mathbf{I}_{(i+1)n} + 2\lambda\Sigma_\epsilon(i)|}}, & \text{if } i \in \{1, \ldots, \mathrm{T}-1\},\ j = 0, \\ 1 - p_{i,0}, & \text{if } i \in \{0, \ldots, \mathrm{T}-1\},\ j = i+1 \\ 1, & \text{if } i = \mathrm{T},\ j = 0. \end{cases}$$

Lemma 11 (Ergodicity): The homogeneous Markov chain $\{\tau_k\}_{k\geq 0}$ with state space $\mathcal{B}$ is ergodic and has a unique invariant distribution $\boldsymbol{\pi} \triangleq \left[\pi(0)\ \pi(1)\ \cdots\ \pi(\mathrm{T})\right] \in \mathbb{R}^{1\times(\mathrm{T}+1)}$ such that $\sum_{i\in\mathcal{B}} \pi(i) = 1$ and $\pi(i) > 0$ for all $i \in \mathcal{B}$.

The communication rate $\mathcal{R}$, here taken as the long-term average number of messages (i.e., state estimates) transmitted from the sensor to the controller, is defined as

$$\mathcal{R} \triangleq \lim_{N\to\infty} \frac{1}{N} \sum_{k=0}^{N-1} \sigma_k.$$

As can be seen in (15), the visit of the Markov chain $\{\tau_k\}_{k\geq 0}$ to the state 0 is analogous to a transmission (i.e., $\sigma_k = 1$) of the state estimate from the sensor to the controller. Then, instead of focusing on σ_k, we can consider the Markov chain $\{\tau_k\}_{k\geq 0}$ to compute the transmission rate. By the ergodic theorem for Markov chains [23, Theorem 5.3], the communication rate $\mathcal{R}$ can, thus, be computed by

$$\mathcal{R} = \pi(0) \triangleq \lim_{N\to\infty} \frac{1}{N} \sum_{k=0}^{N-1} \mathbb{1}_{\{\tau_k = 0\}}$$

where $\pi(0)$ is the empirical frequency of transmissions. With the transition probabilities of this Markov chain, we can give an explicit characterization of the average communication rate of the event-triggered control system.

Theorem 12 (Communication rate): The average communication rate between the sensor and the controller under the stochastic event-based triggering mechanism, proposed in (12)–(14), for a fixed $\lambda > 0$ is given by

$$\mathcal{R} = \frac{1}{1 + \sum_{n=1}^{\mathrm{T}} \prod_{m=0}^{n-1} (1 - p_{m,0})}. \tag{32}$$

The next theorem describes the optimal control law for the event-triggered control system at hand.

Theorem 13 (Certainty-equivalent control): Consider the system (1) and (2), and the problem of minimizing the cost function (19) under the event-based triggering mechanism (12)–(14) for a fixed $\lambda > 0$. Then, there exists a unique admissible optimal control policy

$$\boldsymbol{u}_k = -L_k \mathbf{E}\left[\boldsymbol{x}_k \mid \mathcal{I}^c_k\right] = -L_k \hat{\boldsymbol{x}}^c_{k|k} \tag{33}$$

where

$$L_k = (B^\top S_{k+1} B + R)^{-1} B^\top S_{k+1} A \quad (34)$$

$$S_k = A^\top S_{k+1} A + Q - A^\top S_{k+1} B (B^\top S_{k+1} B + R)^{-1} B^\top S_{k+1} A \quad (35)$$

with initial values $S_N = Q_f$. The minimum value of the cost function is obtained as

$$J_N = \bar{\boldsymbol{x}}_0^\top S_0 \bar{\boldsymbol{x}}_0 + \mathrm{Tr}\,(S_0 X_0) + \sum_{k=0}^{N-1} \mathrm{Tr}\,\big(S_{k+1} W\big) + \sum_{k=0}^{N-1} \mathrm{Tr}\left(P^s_{k|k} M_k\right) + \sum_{k=0}^{N-1} \mathbf{E}\left[\boldsymbol{e}_{k|k}^\top M_k \boldsymbol{e}_{k|k}\right] \quad (36)$$

where $M_k \triangleq L_k^\top (B^\top S_{k+1} B + R) L_k$.

Remark 14: The scheduling decisions in (13) do only depend on independent random variables, and not on past control actions. Based on a similar argument as that provided in [22, Theorem 3.1], the use of the aforementioned scheduling mechanism, which is independent of the past control actions, guarantees certainty equivalence and leads to no dual effect.

As discussed in [9] and [14], under some threshold-based event-triggered scheduling mechanisms, the plant state $\boldsymbol{x}_k$ and the state estimate $\hat{\boldsymbol{x}}^s_{k|k}$ become truncated Gaussian random variables. Similarly, the comparison error $\boldsymbol{e}_{k|k}$, defined in (25), has a truncated Gaussian distribution. As noticed in (36), one should evaluate the covariance of the comparison error to compute the long-run average control loss. However, this covariance cannot be calculated analytically. Wu *et al.* [14], therefore, proposed stochastic scheduling rules, related to (13), to preserve the Gaussianity of the plant state. Next, we will present a lemma to compute the covariance of the comparison error, which is used to quantify the control loss.

Lemma 15 (Gaussianity preservation): The conditional random variable, $\boldsymbol{e}_{k|k} \mid \tau_k = i$, has a Gaussian distribution with zero mean and covariance

$$\Sigma_e(0) = \mathbf{0}_n$$

$$\Sigma_e(i) = \frac{1}{2\lambda}\mathbf{I}_n - \frac{1}{4\lambda^2}\left(A\Sigma_e(i-1)A^\top + \Pi_\eta + \frac{1}{2\lambda}\mathbf{I}_n\right)^{-1}.$$

Using Theorem 13 and Lemma 15, we have the following result to calculate the long-term average control performance.

Theorem 16 (Infinite horizon control performance): Suppose the pairs (A, B) and $(A, W^{1/2})$ are controllable, and the pairs (A, C) and $(A, Q^{1/2})$ are observable. Moreover, suppose that $\lambda > 0$. Then, we have the following:

a) The infinite horizon optimal controller gain is constant

$$L_\infty \triangleq \lim_{k\to\infty} L_k = (B^\top S_\infty B + R)^{-1} B^\top S_\infty A. \quad (37)$$

b) The matrices S_∞ and P^s_∞ are the positive definite solutions of the following algebraic Riccati equations:

$$S_\infty \triangleq A^\top S_\infty A + Q - A^\top S_\infty B (B^\top S_\infty B + R)^{-1} B^\top S_\infty A \quad (38)$$

$$P^s_\infty \triangleq A P^s_\infty A^\top + W - A P^s_\infty C^\top (C P^s_\infty C^\top + V)^{-1} C P^s_\infty A^\top. \quad (39)$$

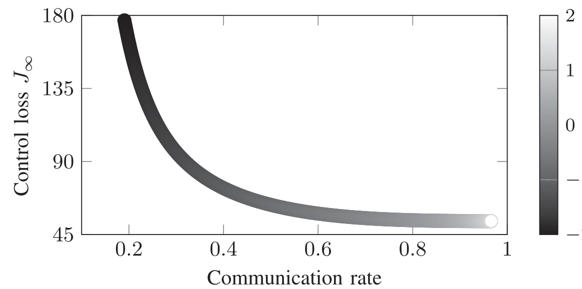

Fig. 2. Tradeoff between the communication rate and the control performance (the scheduling parameter $\log_{10}\lambda$ is illustrated by gray scale).

c) The expected minimum cost converges to the following value:

$$J_\infty \triangleq \lim_{N\to\infty} \frac{1}{N} J_N = \mathrm{Tr}(S_\infty W) + \mathrm{Tr}(F^s_\infty M_\infty) + \sum_{i=1}^{\mathrm{T}} \pi(i) \mathrm{Tr}\Big(M_\infty \Sigma_e(i)\Big) \quad (40)$$

where $F^s_\infty \triangleq (\mathbf{I}_n - K_\infty C) P^s_\infty$, $M_\infty \triangleq L_\infty^\top (B^\top S_\infty B + R) L_\infty$, and $\boldsymbol{\pi} = [\pi(0)\ \pi(1)\ \cdots\ \pi(\mathrm{T})]$ satisfies $\boldsymbol{\pi} = \boldsymbol{\pi}\mathsf{P}$.

Corollary 17: Suppose the pairs (A, B) and $(A, W^{1/2})$ are controllable, and the pairs (A, C) and $(A, Q^{1/2})$ are observable. Then, there exist the following extreme cases.

a) As $\lambda \to \infty$, the communication rate becomes one, and the control loss converges to

$$J_{\lambda\to\infty} \triangleq \mathrm{Tr}(S_\infty W) + \mathrm{Tr}(F^s_\infty M_\infty).$$

b) As $\lambda \to 0$, the communication rate becomes $1/\mathrm{T}+1$, and the control loss converges to

$$J_{\lambda\to 0} \triangleq J_{\lambda\to\infty} + \frac{1}{\mathrm{T}+1} \sum_{i=1}^{\mathrm{T}} \mathrm{Tr}\left(M_\infty \sum_{j=0}^{i-1} A^j \Pi_\eta (A^\top)^j\right).$$

Remark 18: When the time out goes to infinity (i.e., $\mathrm{T} \to \infty$), the discrete-time Markov process appears to be analytically intractable. We, therefore, cannot provide any analytical characterization of the communication rate and control performance in this limiting case.

IV. Numerical Example

In this section, numerical simulations are provided to assess the performance of the stochastic event-triggering algorithm proposed in Section II, and verify the theoretical results presented in Section III. To this end, the system parameters are chosen as follows:

$$A = \begin{bmatrix} 1.2 & 1 \\ 0 & 0.9 \end{bmatrix},\ B = \begin{bmatrix} 0 \\ 1 \end{bmatrix},\ C = \begin{bmatrix} 1 & 0 \end{bmatrix},\ V = 1$$

$$X_0 = W = \begin{bmatrix} 1 & 0.5 \\ 0.5 & 1 \end{bmatrix},\ Q = \begin{bmatrix} 2 & 0.5 \\ 0.5 & 2 \end{bmatrix},\ R = 1.$$

The matrix A has one stable (i.e., 0.9) and one unstable eigenvalue (i.e., 1.2). The time-out interval is set to $\mathrm{T} = 50$.

For various values of λ ranging from 0.01 to 100 (resp. from -2 to 2 in logarithmic scale), we evaluate the communication rate and the control performance as predicted by Theorems 12 and 16, respectively. We can also obtain results on when changing λ has the most effect as demonstrated in Fig. 2. It is observed, for instance, that changing λ from one to large values has minimal effect on the control performance, but nearly doubles the communication frequency. By setting $\lambda = 1$ (resp.

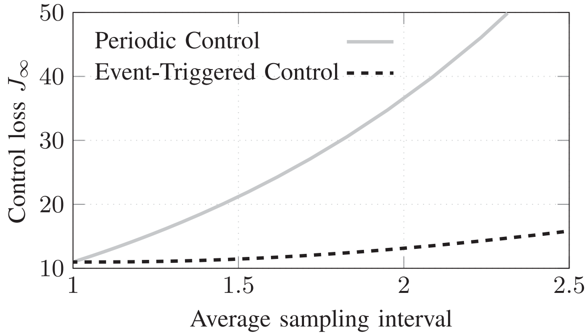

Fig. 3. Comparison of transmission rate (resp. control loss) derived from the analytic expression (32) [resp. (40)] and Monte Carlo simulations.

0 in logarithmic scale), it is possible to reduce the communication between the sensor and the controller by almost 40%, while only slightly sacrificing the control performance of the closed-loop system.

Fig. 3 compares the control loss incurred when the proposed method is applied to a double integrator (see [24, p. 49]) to that obtained when using a standard sampled-data linear-quadratic Gaussian (LQG) controller with varying sampling intervals. Notice that the loss function needs to be discretized; in consequence, the discretization leads to nonzero cross-coupling terms. All theoretical results, presented in the paper, are also valid for this type of loss functions. As seen in Fig. 3, the event-triggered controller proposed in this paper provides significantly better performance than the standard sampled-data LQG controller.

V. Conclusion and Discussions

This paper has focused on the optimal control of stochastic LTI systems, where a stochastic event-based scheduling mechanism governs the communication between the sensor and the controller. The scheduler is colocated at the sensor and employs a Kalman filter. Based on the prediction error, the scheduler decides whether or not to send a new state estimate to the controller. The use of this transmission strategy reduces the communication burden in the channel. It was shown that, in this setup, the optimal controller is the certainty-equivalent controller since the scheduling decisions are not affected by the control policy. Analytical expressions were also provided to quantify the tradeoff between the communication rate and the control performance.

VI. Appendix: Proofs

Proof of Lemma 6: By Assumption 5, the Kalman filter has reached its steady state. Consequently, the Kalman gain K_k and the error covariance matrices, $P^s_{k|k-1}$ and $P^s_{k|k}$, become constant, i.e., K_∞, P^s_∞, and $F^s_\infty = (\mathbf{I}_n - K_\infty C)P^s_\infty$, respectively. Let us define the following random process:

$$\boldsymbol{\eta}_k = K_\infty CA\tilde{\boldsymbol{x}}^s_{k|k} + K_\infty C\boldsymbol{w}_k + K_\infty \boldsymbol{v}_{k+1} \ .$$

Since $\tilde{\boldsymbol{x}}^s_{k|k}$, $\boldsymbol{w}_k$, and $\boldsymbol{v}_{k+1}$ are mutually independent Gaussian vectors with zero mean and covariances F^s_∞, W, and V, respectively, $\boldsymbol{\eta}_k$ is Gaussian with zero mean and covariance

$$\begin{aligned}\Pi_{\boldsymbol{\eta}} &= \mathbf{E}\left[\boldsymbol{\eta}_k\boldsymbol{\eta}_k^\top\right] = \mathbf{E}\left[\left(K_\infty CA\tilde{\boldsymbol{x}}^s_{k|k} + K_\infty C\boldsymbol{w}_k + K_\infty\boldsymbol{v}_{k+1}\right)\right.\\ &\quad\left.\times\left(K_\infty CA\tilde{\boldsymbol{x}}^s_{k|k} + K_\infty C\boldsymbol{w}_k + K_\infty\boldsymbol{v}_{k+1}\right)^\top\right]\\ &= K_\infty\left(C(AF^s_\infty A^\top + W)C^\top + V\right)K_\infty^\top\\ &\overset{(a)}{=} K_\infty\left(CP^s_\infty C^\top + V\right)K_\infty^\top \overset{(b)}{=} K_\infty CP^s_\infty \qquad (41)\end{aligned}$$

where (a) is derived by writing $P^s_\infty \triangleq AF^s_\infty A^\top + W$ while (b) is obtained by replacing $K_\infty^\top$ with $\left(CP^s_\infty C^\top + V\right)^{-1}CP^s_\infty$.

Since $\{\boldsymbol{\eta}_k\}_{k\geq 0}$ are Gaussian random vectors, pairwise independence is equivalent to

$$\mathbf{E}\left[\boldsymbol{\eta}_k\boldsymbol{\eta}_l^\top\right] = \underline{\mathbf{0}}_n, \qquad 0 \leq k < l < \infty.$$

For $k < l$, we have

$$\begin{aligned}\mathbf{E}\left[\boldsymbol{\eta}_k\boldsymbol{\eta}_l^\top\right] &= \mathbf{E}\left[\left(K_\infty CA\tilde{\boldsymbol{x}}^s_{k|k} + K_\infty C\boldsymbol{w}_k + K_\infty\boldsymbol{v}_{k+1}\right)\right.\\ &\quad\left.\times\left(K_\infty CA\tilde{\boldsymbol{x}}^s_{l|l} + K_\infty C\boldsymbol{w}_l + K_\infty\boldsymbol{v}_{l+1}\right)^\top\right]\\ &\overset{(b)}{=} \mathbf{E}\left[\left(K_\infty CA\tilde{\boldsymbol{x}}^s_{k|k} + K_\infty C\boldsymbol{w}_k + K_\infty\boldsymbol{v}_{k+1}\right)\tilde{\boldsymbol{x}}^{s\top}_{l|l}\right]\\ &\quad\times A^\top C^\top K_\infty^\top \overset{(c)}{=} \left(K_\infty C\left(AF^s_\infty A^\top + W\right)(\mathbf{I}_n - K_\infty C)^\top\right.\\ &\quad\left.-K_\infty VK_\infty^\top\right)\left((A - K_\infty CA)^{l-k-1}\right)^\top A^\top C^\top K_\infty^\top\\ &\overset{(d)}{=} \left(K_\infty CP^s_\infty(\mathbf{I}_n - K_\infty C)^\top - K_\infty VK_\infty^\top\right)\\ &\quad\times\left((A - K_\infty CA)^{l-k-1}\right)^\top A^\top C^\top K_\infty^\top \overset{(e)}{=} \underline{\mathbf{0}}_n\end{aligned}$$

where (b) holds since $\boldsymbol{w}_l$ and $\boldsymbol{v}_{l+1}$ are independent of $\hat{\boldsymbol{x}}^s_{k|k}$, $\boldsymbol{w}_k$, and $\boldsymbol{v}_{k+1}$; (c) is obtained by replacing $\hat{\boldsymbol{x}}^s_{l|l}$ with (9) iteratively from l to k and using the fact that $\boldsymbol{w}_k$ and $\boldsymbol{v}_{k+1}$ are independent of $\boldsymbol{w}_{k+1}, \ldots, \boldsymbol{w}_{l-1}$ and $\boldsymbol{v}_{k+2}, \ldots, \boldsymbol{v}_l$; (d) is obtained by writing $P^s_\infty \triangleq AF^s_\infty A^\top + W$; and (e) follows from (41). ■

Lemma 19: Suppose that $\zeta_{k+1}, \zeta_{k+2}, \ldots, \zeta_{k+i}$ is a sample of $\zeta \overset{\text{i.i.d.}}{\sim} \mathrm{Uni}(0,1)$. Define the following events:

$$\begin{aligned}\mathcal{E}_i &\triangleq \left\{\delta_{k+1} = 0, \ldots, \delta_{k+i} = 0\right\}\\ &= \bigcap_{j=0}^{i-1}\left\{\zeta_{k+j+1} \leq e^{-\lambda\langle\boldsymbol{\epsilon}_{k+j}(j),\boldsymbol{\epsilon}_{k+j}(j)\rangle}\right\} \qquad (42)\end{aligned}$$

for all $i \in \{1, 2, \ldots, \mathrm{T}\}$, with the convention that $\mathcal{E}_0$ is a sure event. For any given $\lambda > 0$, the probability of these events $\mathcal{E}_i$, for all $i \in \{1, 2, \ldots, \mathrm{T}\}$, can be computed as

$$\mathbf{P}(\mathcal{E}_i) = \frac{1}{\sqrt{|\mathbf{I}_{in} + 2\lambda\Sigma_\epsilon(i-1)|}}. \qquad (43)$$

Proof of Lemma 19: Assume that $\zeta_{k+1}, \zeta_{k+2}, \ldots, \zeta_{k+i}$ is a sample of $\zeta \overset{\text{i.i.d.}}{\sim} \mathrm{Uni}(0,1)$. Since $\boldsymbol{e}_{k+1|k} = \boldsymbol{\epsilon}_k(i-1)$ when $\tau_k = i-1 \quad \forall i \in \{1, 2, \ldots, \mathrm{T}\}$, the stochastic triggering rule (13) can be rewritten as

$$\delta_{k+i} = \begin{cases} 0, & \text{if } \zeta_{k+i} \leq e^{-\lambda\langle\boldsymbol{\epsilon}_{k+i-1}(i-1),\boldsymbol{\epsilon}_{k+i-1}(i-1)\rangle}\\ 1, & \text{otherwise.}\end{cases}$$

For any given $\lambda > 0$, we compute

$$\begin{aligned}\mathbf{P}(\mathcal{E}_i) &= \mathbf{P}(\delta_{k+1} = 0, \ldots, \delta_{k+i} = 0)\\ &= \mathbf{P}\left(\bigcap_{j=0}^{i-1}\zeta_{k+j+1} \leq e^{-\lambda\langle\boldsymbol{\epsilon}_{k+j}(j),\boldsymbol{\epsilon}_{k+j}(j)\rangle}\right)\\ &= \frac{\int_{\mathbb{R}^{in}} e^{-\frac{1}{2}\chi^\top(i-1)\left(2\lambda\mathbf{I}_{ni} + \Sigma_\epsilon^{-1}(i-1)\right)\chi(i-1)}d\chi}{\sqrt{(2\pi)^{in}|\Sigma_\epsilon(i-1)|}}\\ &= \frac{1}{\sqrt{|\mathbf{I}_{in} + 2\lambda\Sigma_\epsilon(i-1)|}}.\end{aligned}$$

■

Proof of Lemma 10: Using the total law of probabilities and the fact that $\boldsymbol{e}_{k+1} \in \mathbb{R}^n$ [3], we have

$$\begin{aligned}
&\mathbf{P}(\tau_{k+1} \mid \tau_k, \tau_{k-1}, \ldots, \tau_0) \\
&= \int_{\mathbb{R}^n} \mathbf{P}(\tau_{k+1}, \boldsymbol{e}_{k+1} \mid \tau_k, \tau_{k-1}, \ldots, \tau_0) d\boldsymbol{e}_{k+1} \\
&\overset{(a)}{=} \int_{\mathbb{R}^n} \mathbf{P}(\tau_{k+1} \mid \boldsymbol{e}_{k+1}, \tau_k, \tau_{k-1}, \ldots, \tau_0) \\
&\quad \times \mathbf{P}(\boldsymbol{e}_{k+1} \mid \tau_k, \tau_{k-1}, \ldots, \tau_0) d\boldsymbol{e}_{k+1} \\
&\overset{(b)}{=} \int_{\mathbb{R}^n} \mathbf{P}(\tau_{k+1} \mid \boldsymbol{e}_{k+1}, \tau_k) \mathbf{P}(\boldsymbol{e}_{k+1} \mid \tau_k) d\boldsymbol{e}_{k+1} \\
&\overset{(c)}{=} \int_{\mathbb{R}^n} \mathbf{P}(\tau_{k+1}, \boldsymbol{e}_{k+1} \mid \tau_k) d\boldsymbol{e}_{k+1} = \mathbf{P}(\tau_{k+1} \mid \tau_k)
\end{aligned}$$

where (a) and (c) come from the definition of conditional probability, and (b) holds since $\boldsymbol{e}_{k+1}$ depends only on τ_k as described in (29), and τ_{k+1} depends on $\boldsymbol{e}_{k+1}$ and τ_k as described in (13) and (14). In other words, $\{\tau_k\}_{k\geq 0}$ has the Markov property. Consequently, the sequence $\{\tau_k\}_{k\geq 0}$ of random variables with values in $\mathcal{B} = \{0, 1, \ldots, \mathrm{T}\}$ is a Markov chain.

The matrix $\mathsf{P} = \{p_{i,j}\}_{i,j\in\mathcal{B}}$, where

$$p_{i,j} = \mathbf{P}(\tau_{k+1} = j | \tau_k = i)$$

is the transition matrix of the Markov chain (see Fig. 4). The transition probabilities except $p_{i,0}$ for all $i \in \{0, \ldots, \mathrm{T}\}$ and $p_{i,i+1}$ for all $i \in \{0, \ldots, \mathrm{T}-1\}$ are equal to zero as can be seen in (15). Now, we only focus on the nontrivial cases where i can take any value from $\{0, \ldots, \mathrm{T}-1\}$ and $j = 0$, as the remaining cases are evident from the structure of the Markov chain. We first investigate the transition probability $p_{0,0}$. Since $\tau_k = 0$ corresponds to $\delta_k = 1$ as a consequence of (14), we have

$$\begin{aligned}
p_{0,0} &= \mathbf{P}(\tau_{k+1} = 0 \mid \tau_k = 0) \\
&= \mathbf{P}(\delta_{k+1} = 1 \mid \delta_k = 1) \\
&\overset{(a)}{=} \mathbf{P}(\delta_{k+1} = 1) = 1 - \mathbf{P}(\delta_k = 0)
\end{aligned}$$

where (a) is true as δ_k is independent of the random variable $\boldsymbol{\eta}_k$. For any $i \in \{1, \ldots, \mathrm{T}-1\}$, we derive

$$\begin{aligned}
p_{i,0} &= \mathbf{P}\left(\tau_{k+1} = 0 \mid \tau_k = i\right) \\
&\overset{(b)}{=} \mathbf{P}\left(\tau_{k+1} = 0 \mid \tau_k = i, \ldots, \tau_{k-i+1} = 1, \tau_{k-i} = 0\right) \\
&\overset{(c)}{=} \mathbf{P}\left(\delta_{k+1} = 1 \mid \delta_k = 0, \ldots, \delta_{k-i+1} = 0, \delta_{k-i} = 1\right) \\
&\overset{(d)}{=} \mathbf{P}\left(\delta_{k+1} = 1 \mid \delta_k = 0, \ldots, \delta_{k-i+1} = 0\right) \\
&= \frac{\mathbf{P}\left(\delta_{k+1} = 1, \delta_k = 0, \ldots, \delta_{k-i+1} = 0\right)}{\mathbf{P}\left(\delta_k = 0, \ldots, \delta_{k-i+1} = 0\right)} = 1 - \frac{\mathbf{P}\left(\mathcal{E}_{i+1}\right)}{\mathbf{P}\left(\mathcal{E}_i\right)}
\end{aligned}$$

where (b) comes from the Markov property, (c) is the result of (14), and (d) holds since δ_{k-i} is independent of the random variables $\boldsymbol{\eta}_k, \ldots, \boldsymbol{\eta}_{k-i}$. Using the result from Lemma 19, we can straightforwardly compute the transition probabilities as given in the statement of the lemma. Since these transition probabilities are independent of time index $k \geq 0$, $\{\tau_k\}_{k\geq 0}$ is also homogeneous. ■

[3]For simplicity, using a slight abuse of notation, we write $\boldsymbol{e}_{k+1} = \boldsymbol{e}_{k+1|k}$.

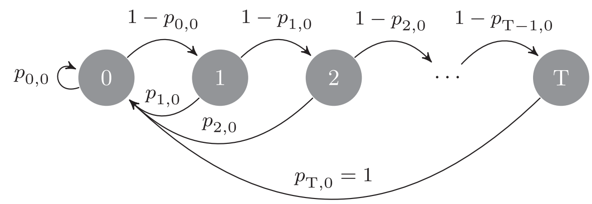

Fig. 4. Transition graph of the Markov chain $\{\tau_k\}_{k\geq 0}$.

Proof of Lemma 11: Since $p_{i,0} \in (0,1)$ for all $i \in \{0, \ldots, \mathrm{T}-1\}$ is true for any $0 < \lambda < \infty$ (see Lemma 10), the chain (see Fig. 4) is evidently irreducible. The chain (see Fig. 4) is also aperiodic because the state 0 has a nonzero probability of being reached for any $0 < \lambda < \infty$ (see Lemma 10). By [23, Theorem 3.3], this irreducible chain with finite state space $\mathcal{B}$ is positive recurrent. Since $\{\tau_k\}_{k\geq 0}$ is irreducible, aperiodic, and positive recurrent, it is also ergodic. As $\{\tau_k\}_{k\geq 0}$ is an irreducible aperodic Markov chain with finitely many states, it has a unique invariant distribution $\boldsymbol{\pi}$ such that $\boldsymbol{\pi}\mathsf{P} = \boldsymbol{\pi}$ and $\boldsymbol{\pi}\underline{\mathbf{1}}_{\mathrm{T}+1} = 1$ (see [25, Corollary 2.11]). ■

Proof of Theorem 12: The proof of this theorem follows similar steps as in [24, p. 98]. ■

Proof of Theorem 13: The proof of this theorem employs a dynamic programming argument(see [26]). Define the optimal value function

$$V_k(\boldsymbol{x}_k) = \min_{\boldsymbol{u}} \mathbf{E}[\boldsymbol{x}_N^\top Q_f \boldsymbol{x}_N + \sum_{t=k}^{N-1} \left(\boldsymbol{x}_t^\top Q \boldsymbol{x}_t + \boldsymbol{u}_t^\top R \boldsymbol{u}_t\right)]. \quad (44)$$

We claim that the solution of the functional (44) is a quadratic function of the form

$$V_k(\boldsymbol{x}_k) = \mathbf{E}\left[\boldsymbol{x}_k^\top S_k \boldsymbol{x}_k \mid \mathcal{I}_k^c\right] + s_k \quad (45)$$

where S_k is a nonnegative definite matrix and s_k is a scalar. Both S_k and s_k are not functions of the applied control inputs $\boldsymbol{u}_0, \ldots, \boldsymbol{u}_{k-1}$. Indeed, this claim is clearly true for $k = N$ with the choice of parameters $S_N = Q_f$ and $s_N = 0$. Suppose that the claim now holds for $k+1$. The value function at time step k is

$$\begin{aligned}
&V_k(\boldsymbol{x}_k) = \min_{\boldsymbol{u}_k} \mathbf{E}\left[\boldsymbol{x}_k^\top Q \boldsymbol{x}_k + \boldsymbol{u}_k^\top R \boldsymbol{u}_k + V_{k+1}(\boldsymbol{x}_{k+1}) \mid \mathcal{I}_k^c\right] \\
&= \mathbf{E}\left[\boldsymbol{x}_k^\top \left(A^\top S_{k+1} A + Q - L_k^\top (B^\top S_{k+1} B + R) L_k\right) \boldsymbol{x}_k \mid \mathcal{I}_k^c\right] \\
&+ \mathrm{Tr}\left(S_{k+1} W\right) + s_{k+1} + \mathbf{E}\left[\tilde{\boldsymbol{x}}_{k|k}^{s\top} L_k^\top (B^\intercal S_{k+1} B + R) L_k \tilde{\boldsymbol{x}}_{k|k}^s\right] \\
&+ \mathbf{E}\left[\boldsymbol{e}_{k|k}^\top L_k^\top (B^\top S_{k+1} B + R) L_k \boldsymbol{e}_{k|k}\right] \\
&+ \min_{\boldsymbol{u}_k} \left(\boldsymbol{u}_k + L_k \hat{\boldsymbol{x}}_{k|k}^c\right)^\top (B^\top S_{k+1} B + R) \left(\boldsymbol{u}_k + L_k \hat{\boldsymbol{x}}_{k|k}^c\right)
\end{aligned}$$

which is obtained by writing $L_k \triangleq (B^\intercal S_{k+1} B + R)^{-1} B^\intercal S_{k+1} A$ and by replacing $\boldsymbol{x}_k$ with $\boldsymbol{e}_{k|k} = \boldsymbol{x}_k - \hat{\boldsymbol{x}}_{k|k}^s - \tilde{\boldsymbol{x}}_{k|k}^s$. Hence, the minimum is obtained for

$$\boldsymbol{u}_k = -L_k \mathbf{E}\left[\boldsymbol{x}_k \mid \mathcal{I}_k^c\right] = -L_k \hat{\boldsymbol{x}}_{k|k}^c. \quad (46)$$

The claim, provided in (45), is also satisfied for the time step k for all $\boldsymbol{x}_k$ if and only if

$$\begin{aligned}
S_k &= A^\top S_{k+1} A + Q - L_k^\top (B^\top S_{k+1} B + R) L_k \\
s_k &= s_{k+1} + \mathrm{Tr}\left(S_{k+1} W\right) + \mathrm{Tr}\left(P_{k|k}^s L_k^\top (B^\top S_{k+1} B + R) L_k\right) \\
&\quad + \mathrm{Tr}\left(L_k^\top (B^\top S_{k+1} B + R) L_k \mathbf{E}\left[\boldsymbol{e}_{k|k} \boldsymbol{e}_{k|k}^\top\right]\right)
\end{aligned}$$

hold. The nonnegative definite matrix S_k is evidently not a function of the applied control inputs $\boldsymbol{u}_0, \ldots, \boldsymbol{u}_{k-1}$. The scalar s_k is also not a function of the applied control inputs $\boldsymbol{u}_0, \ldots, \boldsymbol{u}_{k-1}$ since the comparison error $\boldsymbol{e}_{k|k}$ in (27) is a function of τ_k and $\boldsymbol{\eta}_{k-\tau_k}, \ldots, \boldsymbol{\eta}_{k-1}$ while τ_k in (14) is a function of τ_{k-1} and $\boldsymbol{\eta}_{k-1-\tau_{k-1}}, \ldots, \boldsymbol{\eta}_{k-1}$. Thus, the proof is completed by induction. Since the optimal control law (46) is only a (linear) function of the state estimate $\hat{\boldsymbol{x}}^c_{k|k}$, certainty equivalence is guaranteed. ■

Proof of Lemma 15: The proof of this lemma follows similar arguments to [14, Lemma 4], while also making use of the matrix inversion lemma. ■

Proof of Theorem 16: The proof of (a) and (b) can be found in [26]. We, here, focus on only the proof of (c). Let us define $M_k \triangleq L_k^\top (B^\top S_{k+1} B + R) L_k$. As $N \to \infty$, similar to [26], the expected minimum cost (36) can be written as

$$J_\infty \triangleq \lim_{N\to\infty} \frac{1}{N} J_N = \mathrm{Tr}(S_\infty W) + \mathrm{Tr}\Big(F^s_\infty M_\infty\Big) + \lim_{N\to\infty} \frac{1}{N} \sum_{k=0}^{N-1} \mathbf{E}\Big[\boldsymbol{e}^\top_{k|k} M_k \boldsymbol{e}_{k|k}\Big].$$

The last term in J_∞ can be rewritten as follows:

$$\begin{aligned} &\lim_{N\to\infty} \mathbf{E}\left[\frac{1}{N}\sum_{k=0}^{N-1} \boldsymbol{e}^\top_{k|k} M_k \boldsymbol{e}_{k|k}\right] \\ &= \lim_{N\to\infty} \mathbf{E}\left[\frac{1}{N}\sum_{k=0}^{N-1}\sum_{i=1}^{\mathrm{T}} \boldsymbol{e}^\top_{k|k} M_k \boldsymbol{e}_{k|k} \mathbb{1}_{\{\tau_k = i\}}\right] \\ &= \sum_{i=1}^{\mathrm{T}} \left(\lim_{N\to\infty} \frac{1}{N} \sum_{k=0}^{N-1} \mathrm{Tr}\left((M_k - M_\infty)\Sigma_e(i)\right) \mathbf{P}\left(\tau_k = i\right) \right. \\ &\quad \left. + \lim_{N\to\infty} \frac{1}{N} \sum_{k=0}^{N-1} \mathrm{Tr}\left(M_\infty \Sigma_e(i)\right) \mathbf{P}\left(\tau_k = i\right) \right). \end{aligned} \tag{47}$$

Since the pair (A, B) is controllable and the pair $(A, Q^{1/2})$ is observable, there exists a steady state $S_\infty \in \mathbb{S}^n_{\succeq 0}$ for any initial matrix $S_0 \in \mathbb{S}^n_{\succeq 0}$. As a result, we have: $\lim_{k\to\infty} M_k = M_\infty$ (i.e., elementwise convergence). As seen in [27], the first term of (47) becomes zero while the second term of (47) is

$$\lim_{N\to\infty} \frac{1}{N} \sum_{k=0}^{N-1} \mathrm{Tr}\big(M_\infty \Sigma_e(i)\big) \mathbf{P}\big(\tau_k = i\big) = \mathrm{Tr}\big(M_\infty \Sigma_e(i)\big) \pi(i).$$

■

References

[1] W. Heemels, K. H. Johansson, and P. Tabuada, "An introduction to event-triggered and self-triggered control," in *Proc. IEEE 51st Annu. Conf. Decis. Control*, 2012, pp. 3270–3285.

[2] K. J. Åström and B. Bernhardsson, "Comparison of Riemann and Lebesgue sampling for first order stochastic systems," in *Proc. 41st IEEE Conf. Decis. Control*, 2002, pp. 2011–2016.

[3] M. Rabi, "Packet based inference and control," Ph.D. dissertation, University of Maryland, College Park, MD, USA, 2006.

[4] O. C. Imer and T. Başar, "Optimal control with limited controls," in *Proc. Amer. Control Conf.*, 2006, pp. 298–303.

[5] T. Henningsson, E. Johansson, and A. Cervin, "Sporadic event-based control of first-order linear stochastic systems," *Automatica*, vol. 44, no. 11, pp. 2890–2895, Nov. 2008.

[6] H. Zhang, T. Ma, G.-B. Huang, and Z. Wang, "Robust global exponential synchronization of uncertain chaotic delayed neural networks via dual-stage impulsive control," *IEEE Trans. Syst. Man Cybern. – Part B, Cybern.*, vol. 40, no. 3, pp. 831–844, Jun. 2010.

[7] X. Meng and T. Chen, "Optimal sampling and performance comparison of periodic and event based impulse control," *IEEE Trans. Autom. Control*, vol. 57, no. 12, pp. 3252–3259, Dec. 2012.

[8] X. Meng, V. Gupta, and P. Antsaklis, "Networked state estimation over a shared communication medium," *IEEE Trans. Autom. Control*, vol. 62, no. 4, pp. 1729–1741, Apr. 2017.

[9] B. Demirel, V. Gupta, D. E. Quevedo, and M. Johansson, "On the trade-off between communication and control cost in event-triggered dead-beat control," *IEEE Trans. Autom. Control*, vol. 62, no. 6, pp. 2973–2980, Jun. 2017.

[10] A. Goldenshluger and L. Mirkin, "On minimum-variance event-triggered control," *IEEE Control Syst. Lett.*, vol. 1, no. 1, pp. 32–37, Jul. 2017.

[11] A. Molin and S. Hirche, "On the optimality of certainty equivalence for event-triggered control systems," *IEEE Trans. Autom. Control*, vol. 58, no. 2, pp. 470–474, Feb. 2013.

[12] B. Demirel, E. Ghadimi, D. E. Quevedo, and M. Johansson, "Optimal control of linear systems with limited control actions: Threshold-based event-triggered control," *IEEE Trans. Control Netw. Syst.*, vol. 5, no. 3, pp. 1275–1286, Sep. 2018.

[13] D. Han, Y. Mo, J. Wu, S. Weerakkody, B. Sinopoli, and L. Shi, "Stochtastic event-triggered sensor schedule for remote state estimation," *IEEE Trans. Autom. Control*, vol. 60, no. 10, pp. 2661–2675, Oct. 2015.

[14] J. Wu, X. Ren, D. Han, D. Shi, and L. Shi, "Finite-horizon Gaussianity-preserving event-based sensor scheduling in Kalman filter applications," *Automatica*, vol. 72, pp. 100–107, 2016.

[15] S. Weerakkody, Y. Mo, B. Sinopoli, D. Han, and L. Shi, "Multi-sensor scheduling for state estimation with event-based, stochastic triggers," *IEEE Trans. Autom. Control*, vol. 61, no. 9, pp. 2695–2701, Sep. 2016.

[16] B. Demirel, A. S. Leong, and D. E. Quevedo, "Performance analysis of event-triggered control systems with a probabilistic triggering mechanism: The scalar case," in *Proc. 20th IFAC World Congr.*, 2017, pp. 10084–10089.

[17] F. D. Brunner, D. Antunes, and F. Allgöwer, "Stochastic thresholds in event-triggered control: A consistent policy for quadratic control," *Automatica*, vol. 89, pp. 376–381, Mar. 2018.

[18] Y. Xu and J. P. Hespanha, "Estimation under uncontrolled and controlled communications in networked control systems," in *Proc. 44th IEEE Conf. Decis. Control*, 2005, pp. 842–847.

[19] V. Gupta, A. F. Dana, J. P. Hespanha, R. M. Murray, and B. Hassibi, "Data transmission over networks for estimation and control," *IEEE Trans. Autom. Control*, vol. 54, no. 8, pp. 1807–1819, Aug. 2009.

[20] A. Molin and S. Hirche, "Structural characterization of optimal event-based controllers for linear stochastic systems," in *Proc. IEEE Conf. Decis. Control*, Atlanta, GA, Dec. 2010, pp. 3227–3233.

[21] T. Kaliath, A. Sayed, and B. Hassibi, *Linear Estimation*. Upper Saddle River, NJ, USA: Prentice-Hall, 2000.

[22] C. Ramesh, H. Sandberg, and K. H. Johansson, "Design of state-based schedulers for a network of control loops," *IEEE Trans. Autom. Control*, vol. 58, no. 8, pp. 1962–1975, Aug. 2013.

[23] P. Bremaud, *Markov Chains: Gibbs fields, Monte Carlo Simulation and Queues*, (ser. Texts in Applied Mathematics), Vol. 31. New York, NY, USA: Springer, 1999.

[24] B. Demirel, "Architectures and performance analysis of wireless control systems," Ph.D. dissertation, KTH Royal Institute of Technology, Stockholm, Sweden, May 2015.

[25] E. Çinlar, *Introduction to Stochastic Processes*. Englewood Cliffs, NJ, USA: Prentice-Hall, 1975.

[26] K. J. Åström, *Introduction to Stochastic Control Theory*. NY, New York, USA: Dover, 2006.

[27] B. Demirel, A. S. Leong, V. Gupta, and D. E. Quevedo, "Trade-offs in stochastic event-triggered control," arXiv:1708.02756, 2018.